On the Equation of State of Plasticized Ethyl Cellulose of Varying Degrees of Substitution

Markus Ivo Beck

Hoffmann-La Roche Ltd., Department Vitamins and Fine Chemicals—Product Form Development, CH-4070 Basel, Switzerland

Ivan Tomka*

Institute for Polymers, Swiss Federal Institute of Technology (ETH), CH-8092 Zürich, Switzerland

Received April 5, 1996; Revised Manuscript Received October 30, 1996[⊗]

ABSTRACT: The thermodynamic behavior of various types of plasticized ethyl cellulose with a degree of substitution (DS) in the range of $1.7 \leq DS \leq 2.5$ is presented. Three structurally related polymer−plasticizer systems with different polarities were investigated, namely ethyl cellulose (DS 2.5)−glycerol tributyrate, ethyl cellulose (DS 2.1)−tributyl citrate, and ethyl cellulose (DS 1.7)−diethyl tartrate. The change in the specific volume of the materials was measured over a temperature range of 20−190 °C and a pressure range of 10−100 MPa, and the scaling parameters of the Simha−Somcynsky and the Flory−Orwoll−Vrij equations of state were determined and compared. Good agreement with experiment was obtained for both equations of state. The cohesive energy density (CED) and, in the case of the Simha−Somcynsky equation, the occupied volume fraction (y) of the amorphous mixtures were calculated at thermodynamic equilibrium, that is at temperatures above the relevant glass transition temperature (T_g). The T_g values of the binary mixtures were determined by the dynamic−mechanical method and corrected empirically to yield the low temperature limit of the thermodynamic equilibrium domain. The occupied volume fraction is strongly dependent on presssure and temperature and, above T_g, decreases with increasing amounts of the plasticizer component. As a result of the comparatively narrow pressure range considered in the evaluation of the volumetric data, the magnitude of y was found to be hardly comparable for the three systems investigated, although it accurately reflects the change in the specific volume in each case. The CED generally appears to correlate with the hydrogen bond density of the mixtures and consequently increases with decreasing DS of the polymer component. The CED provides valuable information for the description of intermolecular forces between the segments in the modeled quasi-lattice and may be capable of approximating the size distribution of the unoccupied volume. Hence, both parameters are of outstanding importance in the study of factors that affect the diffusion coefficient of small apolar gas molecules in materials applied as film coatings in product forms of pharmaceutical agents and food additives. In this context, the results of the present contribution were used to discuss the oxygen permeability of plasticized ethyl cellulose in a subsequent paper.

Introduction

Film-forming derivatives of cellulose, such as ethyl cellulose, are used extensively in film coating of solid dosage forms. Since the glassy solidification of these polymers occurs at temperatures markedly above 100 °C, depending on the degree of substitution,[1] plasticizer is usually added in order to produce the desired mechanical properties. The addition of a component of comparatively low molecular weight influences the physicochemical characteristics of these materials significantly.

In the field of protective coatings or permeation selective membranes, the gas barrier properties are of special interest. As a result, a lot of effort has been made to relate the diffusion coefficient of small gas molecules in polymer matrices to parameters such as the unoccupied or free volume and its distribution.[2−7] Despite the fact that the free volume term has been treated in a structurally nonspecified manner in these studies,[2−6] the approaches used give reason to believe that experimental investigations into the pressure and temperature dependence of the specific volume ($P-V-T$ behavior) may provide useful informations for the quantification of these parameters on a physically acceptable basis and also lead to a fuller understanding of transport processes in macromolecular systems. From a more practical standpoint, $P-V-T$ relationships are most helpful tools in the analysis and design of thermoplastic processing procedures such as extrusion or injection molding.

The $P-V-T$ relationships used in this study are hydrostatic equations of state. Although the $P-V-T$ behavior of a polymer is highly dependent on the time scale of the experiment, the spectrum of dilatational relaxations caused by hydrostatic stress fields is comparatively narrow and can be accounted for in experiments conducted on a suitable time scale. The underlying theories are based on statistical−mechanical considerations and serve to describe the thermodynamic behavior of polymeric materials following the principle of corresponding states. Thus, besides being capable of reducing extensive volume data to three characteristic parameters, they also offer the opportunity of modeling specific interactions in a polymer lattice, thereby giving insight into the molecular forces that exist between the polymer chains.

The objective of the present contribution is to evaluate the physical significance of parameters determined by the application of the established equations of state of Simha−Somcynsky[8,9] and Flory[10] to $P-V-T$ data of ethyl cellulose−plasticizer mixtures. While the systems investigated consist of the same structural units, they exhibit a differing hydrogen-bond density. The question then arises as to whether the increasing polarity of the

* Author to whom correspondence should be addressed.
⊗ Abstract published in *Advance ACS Abstracts,* December 15, 1996.

S0024-9297(96)00506-2 CCC: $12.00

mixtures is satisfactorily reflected in increasing cohesive energy and decreasing free volume, as is suggested by group contribution approximations[11] and macroscopic density data.

Theory

The configurational partition function, Z, of an amorphous polymer is computed by modeling a quasi-lattice which consists of a canonical ensemble of N interacting sites occupied by the segments of the polymer chains. The size of these sites is given by the number of volume dependent ("external") degrees of freedom. The equation of state is derived by suitable differentiation, i.e.

$$P = -\left(\frac{\partial A}{\partial V}\right)_{T,N} = kT\left(\frac{\partial(\ln Z)}{\partial V}\right)_{T,N} \tag{1}$$

where P denotes pressure; V, volume; T, temperature; A, the Helmholtz free energy; and Z, the configurational partition function obtained by a summation of Boltzmann's distribution of potential energies over all possible states of the system. The reduced variables of state (designated by a tilde), are defined by the scaling parameters P^*, V^*, and T^* which are computed by adjusting the equation of state to experimental volume data.

$$\tilde{P} = \frac{P}{P^*} \quad \tilde{V} = \frac{V}{V^*} \quad \tilde{T} = \frac{T}{T^*} \tag{2}$$

The various equations of state are commonly subdivided into categories that reflect their differing formalisms, denoted as the cell, hole, and lattice fluid theories.[12] In this study two theories were applied: The well-known cell model of Flory–Orwoll–Vrij (FOV)[10] and the Simha–Somcynsky (SS) hole model.[8] The theories proved to provide reasonable approximations of the data obtained in the temperature and pressure range investigated. The hole model emphasizes the liquid-like character of the polymer melt and has been extended to multicomponent systems by taking the size difference of the components into account.[9] The lattice fluid model, developed by Sanchez–Lacombe,[13] was found to yield significantly less accurate fits and was not considered further. Nevertheless, the refinement of this theory by Panayiotou–Sanchez[14] that factorizes the partition function by explicitly accounting for hydrogen-bond contributions seems to be very promising and has, for instance, been applied successfully to the starch–water system.[15]

The main differences between the SS hole theory and the FOV cell model may be summarized as follows.

(1) The FOV theory ascribes a more solid-like character to the lattice by assuming that the number of lattice sites of the system is independent of temperature. In contrast, Simha and Somcynsky introduce empty lattice sites to account for the thermal expansion and the compressibility of the system. Thereby, an additional entropy contribution arises due to the mixing of occupied and empty lattice sites ("holes"). The volume fractions of occupied (y) and unoccupied ($1 - y$) lattice sites are found by minimizing the Helmholtz free energy with respect to y, which leads to a transcendental equation for y.

(2) Flory describes the interaction energy between the segments as hard sphere repulsion and a soft attraction of unspecified character. The theory yields a cohesive energy that is proportional to the density of the system. In case of the hole theory, the intersegmental energy is approximated by a mean field 6–12 potential of the Lennard–Jones type.

(3) Flory does not *a priori* define a coordination number for the lattice, whereas Simha–Somcynsky specify a coordination number of 12. The Madelung coefficients A and B in eq 3 include the contribution of non-nearest neighbor shells to the intermolecular energy.

The underlying assumptions of the theories were detailed in the original papers and, therefore, only the aspects relevant to the present discussion will be considered further.

The Simha–Somcynsky equation of state assumes the form

$$\frac{\tilde{P}\tilde{V}}{\tilde{T}} = \frac{1}{1-\eta} + \frac{2y}{\tilde{T}(y\tilde{V})^2}\left(\frac{A}{(y\tilde{V})^2} - \frac{B}{2}\right) \tag{3}$$

where $A = 1.011$ and $B = 2.409$. It is completed by the minimum condition on the Helmholtz free energy with respect to the occupied volume fraction, y:

$$\frac{\langle r\rangle}{3\langle c\rangle}\left[\frac{\langle r\rangle - 1}{\langle r\rangle} + \frac{1}{y}\ln(1-y)\right] = \frac{\eta - 1/3}{1-\eta} + \frac{y}{6\tilde{T}(y\tilde{V})^2}\left(B - \frac{3A}{(y\tilde{V})^2}\right) \tag{4}$$

where

$$\eta = 2^{-1/6}y(y\tilde{V})^{-1/3}$$

The reduced variables of state are defined by the scaling parameters as follows:

$$\tilde{P} = \frac{Prv^*}{\mathrm{qz}\varepsilon^*} \quad \tilde{V} = \frac{v}{v^*} \quad \tilde{T} = \frac{ckT}{\mathrm{qz}\varepsilon^*} \tag{5}$$

The molecule is characterized by the number of segments, r, and the number of external degrees of freedom, $3c$ (high polymers: $r \to \infty$ and $3c = r$; consistent analogue for oligomers: $3c = r + 3$).[9] In the case of multicomponent systems, defined by the component mole fractions, x_i, the scaled equation of state is formally identical to that of a homogenous fluid, and the average values for $\langle c\rangle$ and $\langle r\rangle$ are defined explicitly by $\langle c\rangle = \sum x_i c_i$ and $\langle r\rangle = \sum x_i r_i$.[9,16] The number of nonbonded nearest neighbor segments per chain is given by qz (qz $= r(z - 2) + 2$), where z is the coordination number of the lattice. The intersegmental interactions are specified by the maximum attractive energy parameter, ε^*, and the segmental repulsion volume, v^*. The cohesive energy density, E_{coh}, of the system becomes

$$E_{\mathrm{coh}} = \frac{yP^*}{2\tilde{V}}\left(\frac{B}{(y\tilde{V})^2} - \frac{A}{(y\tilde{V})^4}\right) \tag{6}$$

The equation of state derived by Flory[10] is given by

$$\frac{\tilde{P}\tilde{V}}{\tilde{T}} = \frac{\tilde{V}^{1/3}}{\tilde{V}^{1/3} - 1} - \frac{1}{\tilde{V}\tilde{T}} \tag{7}$$

with the reduced variables of state defined by the scaling parameters as follows

$$\tilde{P} = \frac{2P(v^*)^2}{s\eta} \quad \tilde{V} = \frac{v}{v^*} \quad \tilde{T} = \frac{2v^*ckT}{s\eta} \tag{8}$$

An *r*-mer molecule is characterized by the mean interaction between a segment pair, η; the hard core or net volume of a segment, v*; the average number, s, of nonbonded nearest neighbors per segment ($s = qz/r$ where $qz = r(z - 2) + 2$); and the total number of external degrees of freedom, $3cr$, per molecule. The cohesive energy density, E_{coh}, is given by

$$E_{coh} = P^*/\tilde{v}^2 \tag{9}$$

Experimental Section

Materials. The polymers used in this study were ethyl celluloses with varying degrees of substitution (DS). The DS was determined by a modification of the Zeisel method (ASTM D-914−50), which is described by Jullander.[17] The derivatives investigated had DS values of 2.48 (Hercules ethyl cellulose N 50), 2.12, and 1.69; in the following section they are denoted as ec-2.5, ec-2.1, and ec-1.7. The latter two products are not generally available and were purchased from Aqualon East BV (Rijswijk, The Netherlands). The polymers were analyzed by wide angle X-ray scattering (WAXS), heat flow calorimetry (DSC), dynamic−mechanical thermal analysis (DMTA) and pressure−volume−temperature ($P-V-T$) measurements. The results give reason to believe that the materials are amorphous and, on the large scale, reasonably uniform in substitution.[18]

The plasticizers glycerol tributyrate (gtb) and diethyl tartrate (det) were purchased from Fluka Chemie AG (Buchs, Switzerland). Tributyl citrate (tbc) is a product (Morflex 4) of Morflex, Inc. (Greensboro, NC). The plasticizers were used without further treatment.

Sample Preparation. For DMT and $P-V-T$ analysis, the samples were prepared by thermoplasticizing the premixed polymer−plasticizer systems at 50−180 °C for 5 to 10 min in a Brabender kneader (Brabender OHG, Typ W 30). The mixing temperature depended strongly on the viscosity of the melt. The materials were then compression molded (Given P. H. I. PW-2200) to regularily shaped bodies (dimensions: 40 × 12 × 1 mm) at 185 °C, cooled at a rate of 10 °C/min, dried, and annealed for 4 weeks at room temperature over P_2O_5. Mixtures with large amounts of plasticizer were prepared by dissolving the components in highly volatile solvents. The viscous solutions were cast onto glass plates and the solvent was allowed to evaporate at room temperature (further drying as described above). The solvents selected were dichloromethane/ethanol (4/1) v/v for ec-1.7/det, toluene/ethanol (4/1) v/v for ec-2.1/tbc and distilled tetrahydrofuran for ec-2.5/gtb.

Dynamic−Mechanical Thermal Analysis. The mechanical measurements were carried out over a temperature range of 20−200 °C (max.) using an Mk II DMT analyzer (Polymer Laboratories Ltd.) at a heating rate of 2 °C/min. The upper temperature was limited by the rapidly decreasing mechanical stability of the plasticized samples above T_g. All experiments were performed under a dry nitrogen atmosphere. In the dual cantilever bending mode, an oscillation frequency of 1 Hz (strain: 32−64 μm) was applied to the center of the sample (5 mm free length between driving shaft and frame). The glass transition temperature was determined from the maximum of the loss tangent (tan δ).

Pressure−Volume−Temperature Analysis. The measurements were performed using a $P-V-T$ apparatus constructed by Gnomix Research, Inc. The change in the specific volume was recorded over a temperature range of 25−200 °C and a pressure range of 10−100 MPa in the ITS (isothermal standard) mode. Starting at 25 °C and 10 MPa, the sample was exposed to a stepwise increase of hydrostatic pressure under isothermal conditions. In order to account for time dependent dilatational relaxations, the sample was held under constant conditions for 60 s before the specific volume was recorded. After reaching 100 MPa, the pressure was reduced back to 10 MPa and the sample heated to the next nominal temperature at a rate of approximately 1 °C/min.

Density Measurement. The density of the mixtures was determined by weighing the dry samples in air and in paraffin oil at 25 °C. The density of the oil was measured with the aid of a standardized glass body of known volume (accessory equipment FNR 33360 for Mettler analytical balance AE 260).

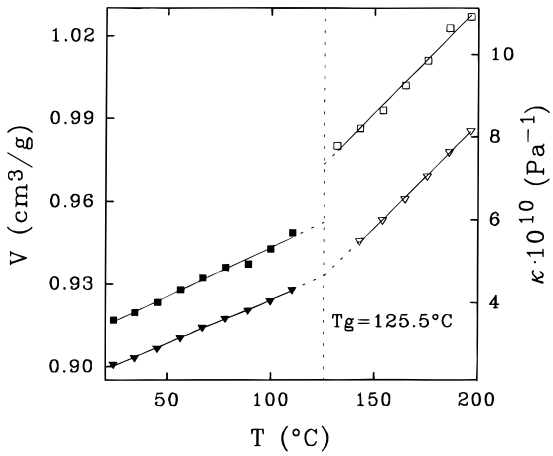

Figure 1. Specific volume, V, (▼, ▽), and compressibility, κ, (■, □), of pure ethyl cellulose (DS 2.5) versus temperature, T.

Results and Discussion

Thermal and Thermomechanical Characterization. The equations of state reviewed only hold at thermodynamic equilibrium and, therefore, can only be applied to the volume data of polymer melts. In the case of the amorphous systems investigated, the glass transition temperature was therefore taken as the low temperature limit of the experimental data used in the evaluation of the characteristic parameters.

Ethyl cellulose−plasticizer mixtures with plasticizer amounts exceeding a weight fraction of 0.15 did not show a distinct glass transition as measured by heat capacity or specific volume changes and the loss tangent maximum determined by DMTA was the only method capable of providing a glass transition temperature. It has to be pointed out that the dynamic−mechanical method deals with long-range shear motions, and therefore does not characterize the thermodynamic state of the sample directly. According to the model of a second-order transition, glass formation is associated with a reduction of the number of degrees of freedom affecting the volumetric properties and, hence, is phenomenologically indicated by a discontinuity of the thermal expansivity and the compressibility (Figure 1). However, previous results suggest an empirical correlation of the T_g values obtained by the different methods mentioned above.[18] This offers an opportunity for the estimation of a glass transition temperature that characterizes the volume recovery of the system, on the basis of the T_g obtained from DMTA. In this manner, the dynamic−mechanical T_g values measured (Figure 2) were shifted downward by 30 °C, yielding the low-temperature limit of the thermodynamic equilibrium domain.

In order to represent the volume−temperature curve, it was found convenient to ignore the slight variations of the thermal expansivity as a function of temperature compared with the jump in this property on passing T_g. Therefore, the expansivities are reported as constants below and above T_g (Table 1). Depending on the hydrogen-bond density, the materials had decreasing thermal expansivity and compressibility with decreasing DS in the liquid, as well as in the glassy, state. Whereas highly substituted ethyl cellulose shows volumetric

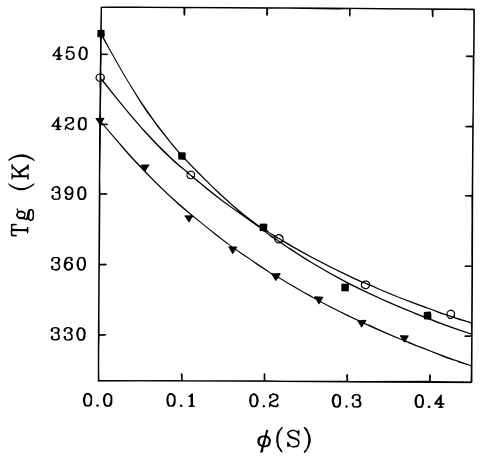

Figure 2. Glass transition temperature, T_g, of plasticized ethyl cellulose obtained from DMT analysis versus volume fraction, $\phi(S)$, of the plasticizer: (■) ec-1.7/det, (○) ec-2.1/tbc, (▼) ec-2.5/gtb, (—) theory according to eq 10.

Table 1. Density, ρ, Glass Transition Temperature, T_g, Compressibility, $\kappa = -(\partial(\ln V)/\partial P)_T$, and Thermal Expansivity, $\alpha = (\partial(\ln V)/\partial T)_P$, of Various Types of Ethyl Cellulose at 0.1 MPa

	ρ (g/cm^3)	T_g	k·10^{10} (Pa^{-1})		a·10^4 (K^{-1})	
DS	T = 25 °C	(°C)	T = 25 °C	T = 175 °C	$T < T_g$	$T > T_g$
2.5	1.114	125.5	3.56	9.94	3.35	8.03
2.1	1.152	143.6	3.49	8.85	3.18	7.31
1.9	1.167	151.4	3.40	8.05	3.05	6.95
1.7	1.186	156.2	3.27	7.04	2.84	6.62

Table 2. Parameters for the Calculation of the Dynamic-Mechanical Glass Transition Temperature of Ec/Plasticizer Mixtures According to Eq 10

system	T_g(P) (K)	k_1	k_2 (K)
ec-1.7/det	458.8	4.18	293.4
ec-2.1/tbc	440.0	3.37	297.7
ec-2.5/gtb	421.7	3.06	275.4

properties comparable to the polyolefins, less etherified derivatives more closely resemble the polyacrylates.

Equation 10 was used to fit the measured glass transition temperatures of the binary mixtures as a function of the volume fraction, $\phi(S)$, of the plasticizer.[19] T_g(P) denotes the glass transition temperature of the pure polymer:

$$T_g = \frac{[1 - \phi(S)]T_g(\mathrm{P}) + k_1\phi(S)k_2}{[1 - \phi(S)] + k_1\phi(S)} \qquad (10)$$

Since the $P-V-T$ measurement is only capable of recording the changes in sample volume, the density of the mixtures at room temperature is required as a reference value for the analysis of the absolute volume data. From Figure 3 it can be seen that the density reaches a maximum at small volume fractions of the plasticizer. Due to increased glass transition temperatures, mixtures with small amounts of plasticizer exhibit increased unrelaxed volume portions at room temperature, thereby indicating an excess free or unoccupied volume fraction. As the temperature is raised, the density maximum is less pronounced and shifts to smaller volume fractions of the plasticizer. Finally, at temperatures above the T_g of the pure polymer, it disappears completely (Figure 4). A macroscopic phase separation was observed for the system ec-2.1/tbc in the composition range of $0.7 < \phi(S) < 1.0$.

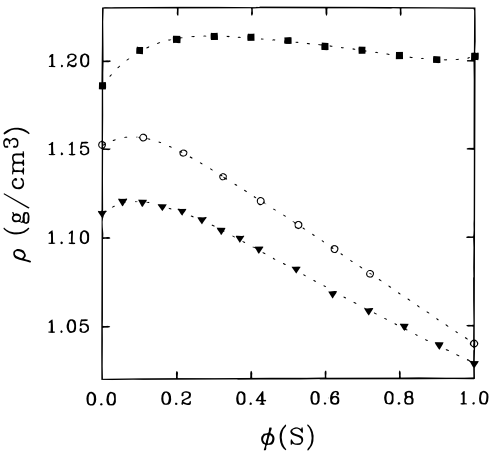

Figure 3. Density, ρ, of ec/plasticizer mixtures versus volume fraction, $\phi(S)$, of the plasticizer at 25 °C and 0.1 MPa: (■) ec-1.7/det, (○) ec-2.1/tbc, (▼) ec-2.5/gtb.

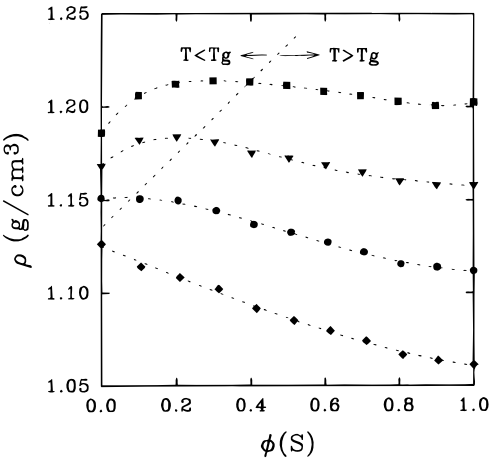

Figure 4. Density, ρ, of the mixture ec-1.7/det versus volume fraction, $\phi(S)$, of the plasticizer at 0.1 MPa: (■) 25 °C, (▼) 75 °C, (●) 125 °C, and (◆) 175 °C.

The concentration dependence of the compressibility is shown in Figure 5. As the plasticizer exceeds a concentration that yields mixtures with a T_g below the temperature of the observed isotherm, the compressibility shows a discontinuity with respect to composition. Mixtures at temperatures below T_g provide significantly smaller compressibilities. This behavior indicates the partially frozen character of the amorphous lattice which has incompressible portions of free volume. Recent data have shown that these unrelaxed volume portions may be the origin of the increased sorption of apolar gases as oxygen.[1] Such penetrants do not interact with the polymer in the sense of swelling or solubilizing the host matrix and, therefore, are only capable of occupying pre-existing molecular voids in the lattice.

Typical $P-V-T$ data for a glass-forming polymer are illustrated in Figure 6. The compressibility was calculated by fitting third-order polynomials to the volume data along the isotherms (Figure 6a). This method provides more accurate values when compared with those computed from the scaling parameters (Figures 7a,b).

The isobaric plot (Figure 6b) offers the possibility of computing the pressure dependence of T_g, which is often investigated to address the question as to whether or not the observed glass transition can be treated as a second-order transition. Despite the fact that experi-

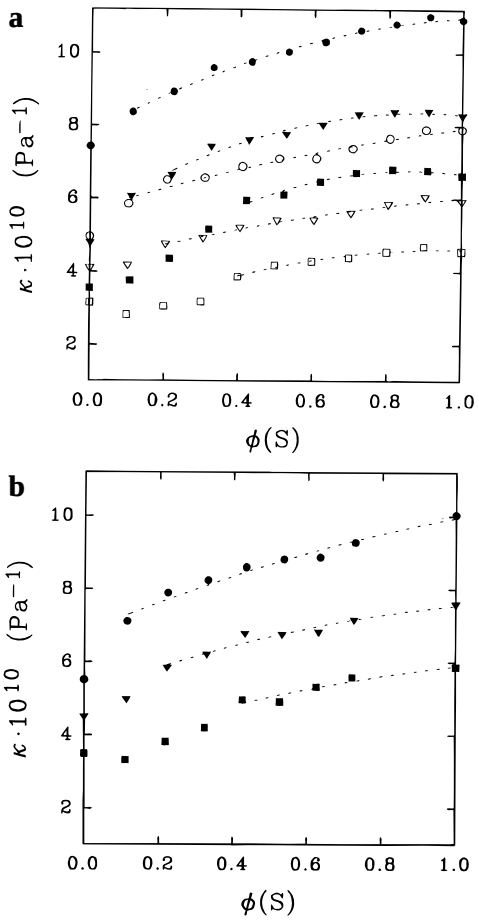

Figure 5. (a) Compressibility, κ, at 0.1 MPa of ec/plasticizer mixtures (filled symbols, ec-2.5/gtb; open symbols, ec-1.7/det) versus volume fraction, $\phi(S)$, of the plasticizer: (■, □) 25 °C, (▼, ▽) 75 °C, (●, ○) 125 °C, (--) $T > T_g$. (b) Compressibility, κ, at 0.1 MPa of mixtures of ec-2.1 and tbc versus volume fraction, $\phi(S)$, of the plasticizer: (■) 25 °C; (▼) 75 °C; (●) 125 °C; (--) $T > T_g$.

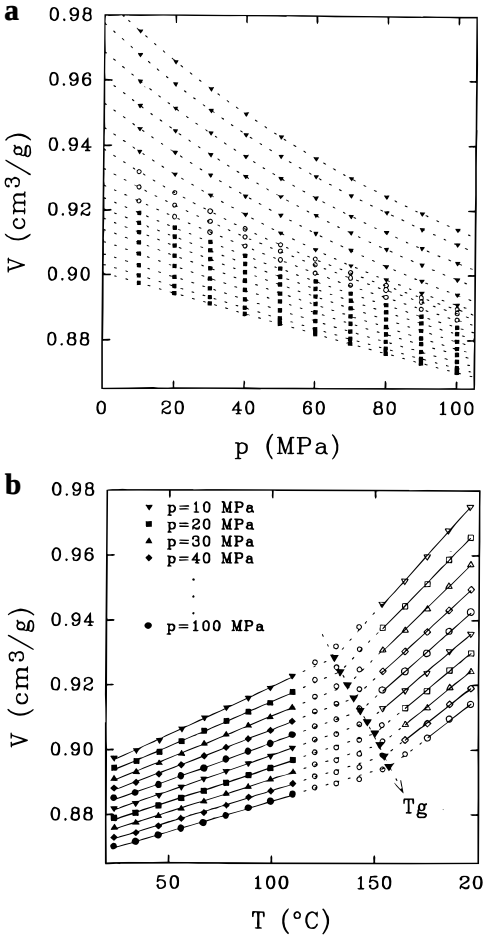

Figure 6. (a) Isotherms of the specific volume, V, of ec-2.5 versus pressure, P: (▼) 143−196 °C ($T > T_g$); (○) 110−132 °C (T ~ T_g); (■) 24−100 °C (T < T_g); (--) third-order polynomial fits. (b) Isobars of the specific volume, V, of ec-2.5 versus temperature, T (pressures as indicated): Filled (open) symbols are volume data below (above) T_g (▼). (○) data points in the region of T_g, (—) linear fits.

ments generally provide evidence of a kinetic, and thus formation-history dependent, event, extended theoretical attempts have been made to describe the glassy solidification in terms of thermodynamic variables. Comprehensive reviews concerning the theoretical treatment of glass formation and glassy behavior are given by Haward and McKenna.[20,21] For example, the Gibbs−Dimarzio model predicts the existence of an underlying, true, second-order transition at a temperature T_2 ($T_2 < T_g$), where the configurational entropy of the supercooled amorphous phase becomes zero.[22] Other approaches describe the nonequilibrium nature of the glassy state by a free energy function and thereby introduce one (or more) additional internal ordering parameters.[20,23] The present contribution is restricted to showing that the magnitude of the pressure dependence of T_g of the ethyl celluloses investigated is apparently in accordance with the Ehrenfest ratio I, which is derived from the volume continuity at the glass transition temperature. Free volume considerations, on the other hand, suggest that the magnitude of the pressure dependence is correlated with the total amount of free volume, as is qualitatively indicated by the compressibility of the polymer melts (Table 3).

Equation of State. The $P-V-T$ surfaces obtained from experiment were analyzed using the equations of state according to Simha−Somcynsky (eqs 3 and 4) and Flory−Orwoll−Vrij (eq 7). In order to evaluate the scaling parameters of the mixtures, the Simha−Somcynsky theory extended to multicomponent fluids was applied.[9] In this context, the average number, $\langle r \rangle$, of segments per molecule had to be fixed with respect to the magnitude of r_1 for the low molecular weight component. The latter was determined by carrying out an iterative procedure: Starting with $r_1 \rightarrow \infty$, the scaling parameters were adjusted according eqs 3 and 4. With known P^*, V^*, T^* and $M(S)$, a successive r_1 was evaluated using the coupled eqs 11a−c. This two-step procedure was repeated until r_1 became consistent with the following conditions:

$$M_1 = c_1 R T^*/(r_1 P^* V^*) \tag{11a}$$

where

$$3c_1 = r_1 + 3 \tag{11b}$$

and

$$M(S) = r_1 M_1 \tag{11c}$$

$M(S)$ and M_1 denote the molecular weight of the plasticizer and the segments of the plasticizer molecule, respectively. Due to the lack of reliable data for the molecular weight of the ethyl celluloses investigated,

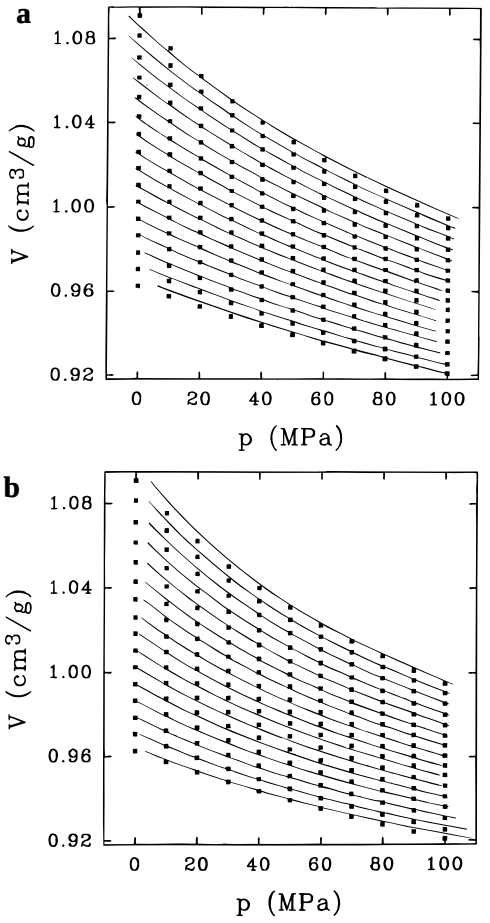

Figure 7. (a) Isotherms of tributyl citrate in the temperature range of 25−185 °C (increments $\Delta T \sim 10.5$ °C): (■) experiment, (—) theory according to Simha−Somcynsky; $r = 6.0$, $P^* = 676.8$ MPa, $V^* = 0.9430$ cm^3/g, $T^* = 9201$ K. (b) Isotherms of tributyl citrate in the temperature range of 25−185 °C (increments $\Delta T \sim 10.5$ °C). (■) experiment, (—) theory according to Flory−Orwoll−Vrie; $P^* = 431.4$ MPa, $V^* = 0.8183$ cm^3/g, $T^* = 6605$ K.

Table 3. Pressure Dependence, $\partial T_g/\partial P$, of the Glass Transition Temperature in the Range of 0−100 MPa, Ehrenfest Ratio I, $(\Delta\kappa/\Delta\alpha)_{T=T_g}$, and Compressibility, κ, of Various Polymer Melts

polymer	$\partial T_g/\partial P$ (K/MPa)	$\Delta\kappa/\Delta\alpha$ (K/MPa) $T = T_g$	κ (Pa^{-1}) $T = 175$ °C
ec-2.5	0.30	0.30	9.9
ec-2.1	0.27	0.26	8.8
zein[a]	0.18	0.19	4.2

[a] Protein from *zea mais*.[24]

$\langle r\rangle$ could not be calculated according the simple relation $\langle r\rangle = \sum x_i r_i$ with x_i representing the molar fractions of the components. Therefore, the following procedure was used: The total number of segments, N, in the mixture can be evaluated by taking into account the weight fractions $w(S)$ and $w(P)$ and the molecular weights, M_1 and M_2, of the segments of the plasticizer and the polymer.

$$N = w(S)/M_1 + w(P)/M_2 \tag{12}$$

M_2 is defined by the scaling parameters obtained from $P-V-T$ data on the pure polymer melts:

$$M_2 = RT^*/(3P^*V^*) \tag{13}$$

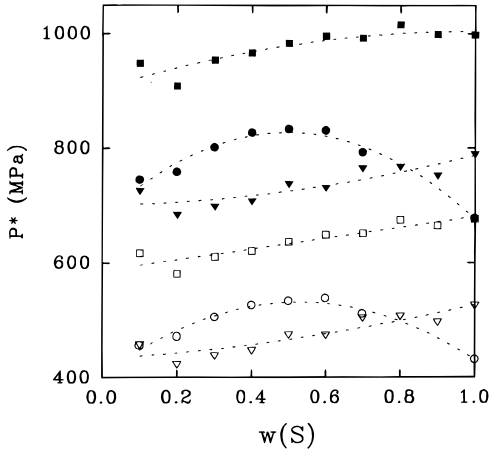

Figure 8. Scaling parameter P^* of ec/plasticizer mixtures according to the Simha−Somcynsky (filled symbols) and Flory−Orwoll−Vrie (open symbols) theories: (■, □) ec-1.7/det, (●, ○) ec-2.1/tbc; (▼, ▽) ec-2.5/gtb.

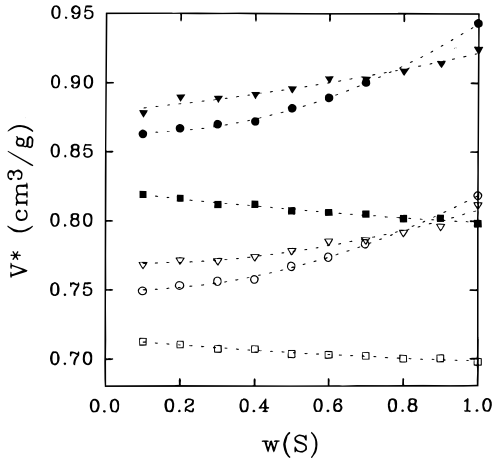

Figure 9. Scaling parameter V^* of ec/plasticizer mixtures according to the Simha−Somcynsky (filled symbols) and Flory−Orwoll−Vrie (open symbols) theories: (■, □) ec-1.7/det, (●, ○) ec-2.1/tbc; (▼, ▽) ec-2.5/gtb.

Very few isotherms could be measured in the region between T_g and the temperature of thermal decomposition, particularly for the derivatives with limited substitution. For this reason, the scaling parameters of the pure polymers obtained turned out to be less significant. A way of overcoming this complication was to utilize an average value, $\langle M_2\rangle$, of the three derivatives for all three systems investigated. In this manner, $\langle M_2\rangle$ was calculated to be 65 g/mol.

In order to derive $\langle r\rangle$ for the mixtures, it was assumed that the total number of molecules in the mixture could be approximated by the number of plasticizer molecules, $N(S)$. Accordingly, $\langle r\rangle$ is defined as follows:

$$\langle r\rangle = N/N(S) \tag{14}$$

The fit of the Simha−Somcynsky equation to the experimental $P-V-T$ data was carried out by a Levenberg−Marquardt procedure that allowed a simultaneous determination of all parameters.[25] A simple, nonlinear least square fit was performed in order to obtain the scaling parameters according to Flory. The results are displayed in Table 4 and Figures 8, 9, and 10. As a measure of the accuracy of the fits, the mean deviation of the specific volume, ΔV, was calculated, where n is the number of data points:

Table 4. Scaling Parameters of Ec/Plasticizer Mixtures According to the Equation of State of Simha−Somcynsky and Flory−Orwoll−Vrij[a]

		Simha−Somcynsky					Flory−Orwoll−Vrij			
$w(S)$	T_u (°C)	$\langle r \rangle$	P^* (MPa)	V^* (cm^3/g)	T^* (K)	$\Delta V \cdot 10^4$ (cm^3/g)	P^* (MPa)	V^* (cm^3/g)	T^* (K)	$\Delta V \cdot 10^4$ (cm^3/g)
Ethyl Cellulose (DS 2.5)/Glycerol Tributyrate										
0.10	75	48.7	725.5	0.8779	10376	13.5	458.6	0.7628	7122	13.4
0.20	55	25.4	684.0	0.8895	10447	12.6	423.9	0.7716	7154	11.9
0.30	35	17.6	698.1	0.8886	9739	10.6	439.2	0.7713	6754	14.4
0.40	25	13.8	707.5	0.8916	9398	11.4	448.0	0.7742	6573	17.7
0.50	25	11.4	737.2	0.8955	9029	8.2	475.3	0.7784	6395	18.9
0.60	25	9.9	730.9	0.9030	8789	7.7	474.9	0.7853	6273	20.6
0.70	25	8.8	764.7	0.9027	8405	8.8	504.7	0.7864	6082	23.2
0.80	25	8.0	767.2	0.9085	8289	7.5	507.9	0.7917	6029	24.9
0.90	25	7.3	751.9	0.9141	8118	6.2	497.3	0.7960	5905	23.5
1.00	25	6.8	789.0	0.9242	8093	9.5	527.4	0.8063	5954	23.7
Ethyl Cellulose (DS 2.1)/Tributyl Citrate										
0.10	95	55.9	743.9	0.8625	11541	14.6	455.8	0.7492	7862	11.4
0.20	65	28.2	758.2	0.8670	10721	15.0	471.3	0.7532	7382	12.1
0.30	45	18.9	800.1	0.8698	10083	13.4	505.5	0.7563	7034	10.2
0.40	35	14.3	826.0	0.8716	9491	6.7	525.7	0.7578	6670	11.4
0.50	25	11.6	832.0	0.8817	9365	10.5	533.1	0.7672	6651	20.2
0.60	25	9.7	829.8	0.8890	9075	10.6	537.7	0.7738	6499	15.2
0.70	25	8.4	791.8	0.9003	9078	10.6	511.5	0.7833	6520	13.7
1.00	25	6.0	676.8	0.9430	9201	12.3	431.4	0.8183	6605	18.2
Ethyl Cellulose (DS 1.7)/Diethyl Tartrate										
0.10	105	32.7	948.2	0.8189	10856	8.4	616.8	0.7124	7552	10.1
0.20	75	16.9	908.1	0.8163	10544	9.0	581.1	0.7103	7417	10.9
0.30	55	11.6	953.5	0.8119	10052	8.9	610.6	0.7073	7167	9.8
0.40	35	9.0	966.3	0.8120	9666	9.7	620.7	0.7074	6954	7.9
0.50	25	7.4	983.4	0.8072	9306	10.5	636.5	0.7037	6764	9.6
0.60	25	6.3	995.7	0.8061	9081	10.8	649.0	0.7031	6662	9.8
0.70	25	5.6	992.6	0.8050	8888	11.4	651.5	0.7023	6570	9.1
0.80	25	5.0	1015.9	0.8016	8559	9.8	674.7	0.7002	6393	8.2
0.90	25	4.5	998.9	0.8019	8474	11.6	664.8	0.7004	6356	9.1
1.00	25	4.2	997.9	0.7981	8281	9.1	676.5	0.6977	6268	7.1

[a] The equations were applied over a pressure range of 0−100 MPa and a temperature range of T_u − 185 °C. T_u is the approximate low-temperature limit of the thermodynamic equilibrium domain; $w(S)$ is the weight fraction of the plasticizer.

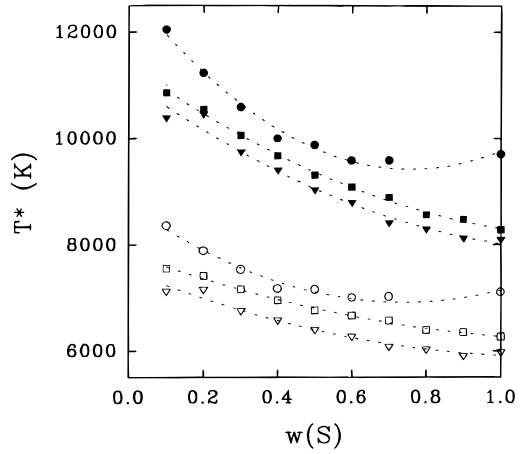

Figure 10. Scaling parameter T^* of ec/plasticizer mixtures according to the Simha−Somcynsky (filled symbols) and Flory−Orwoll−Vrie (open symbols) theories: (■, □) ec-1.7/det; (●, ○) ec-2.1/tbc, shifted by +500 K; (▼, ▽) ec-2.5/gtb.

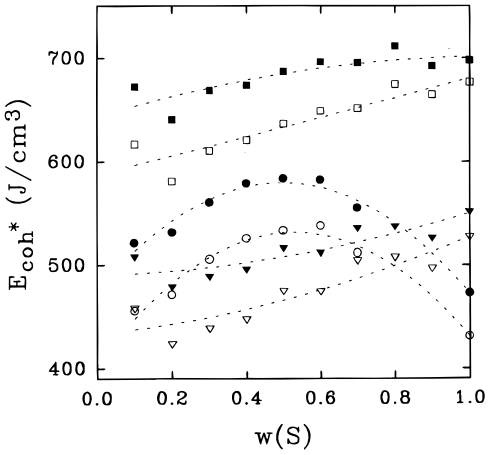

Figure 11. Cohesive energy density, E_{coh}^*, of ec/plasticizer mixtures according to the Simha−Somcynsky (filled symbols) and Flory−Orwoll−Vrie (open symbols) theories versus the weight fraction, $w(S)$, of the plasticizer: (■, □) ec-1.7/det, (●, ○) ec-2.1/tbc, (▼, ▽) ec-2.5/gtb.

$$\Delta V = \sqrt{\sum_{i=1}^{n} (V_{exp} - V_{theor})^2 / n} \qquad (15)$$

Although the computed scaling parameters fit the volume data quite well over a wide range of temperature, the slope of the isotherms is very sensitive to slight variations in the specific volume. Close to the high- and low-temperature limits, deviations from experimental data become significant and the theoretical isotherms no longer satisfactorily represent the compressibility of the materials (Figures 7a,b).

In mixtures with decreasing amounts of plasticizer, the scaling parameters are applied over a narrower temperature range. Hence, it is surprising that the accuracy of the fits does not improve. As a matter of fact, the Simha−Somcynsky equation strikingly shows even less accuracy at low plasticizer concentrations (Table 4).

Cohesive Energy Density and Occupied Volume. With $v = v^*$ ($y = 1$), the hypothetical cohesive energy density, E_{coh}^*, of a lattice possessing maximum density can be calculated (Figure 11). The obtained values correlate fairly well with the increasing polarity of the

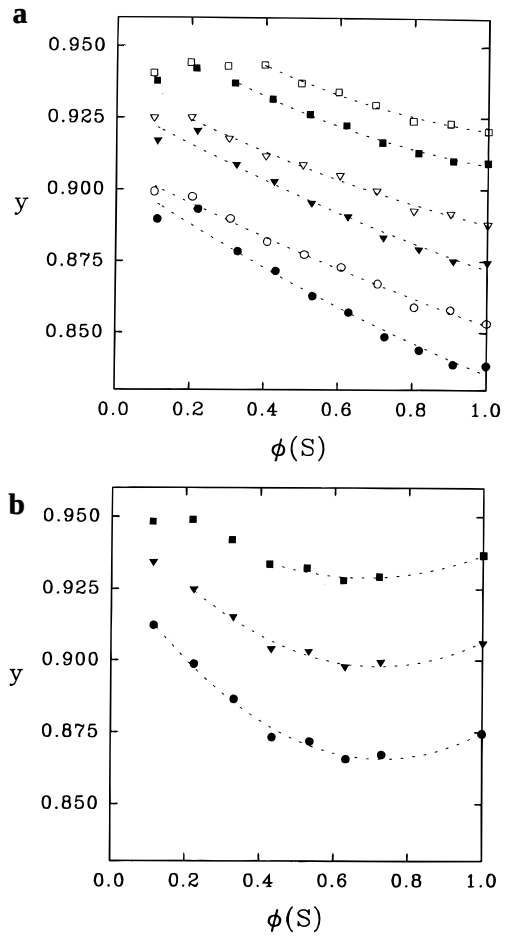

Figure 12. (a) Occupied volume fraction, y, ($p = 0.1$ MPa) of ec/plasticizer mixtures versus volume fraction, $\phi(S)$, of the plasticizer (filled symbols, ec-2.5/gtb; open symbols, ec-1.7/det): (■, □) 25 °C, (▼, ▽) 75 °C, (●, ○) 125 °C, (--) $T > T_g$. (b) Occupied volume fraction, y, ($p = 0.1$ MPa) of mixtures of ec-2.1 and tbc versus volume fraction, $\phi(S)$, of the plasticizer: (■) 25 °C; (▼) 75 °C; (●) 125 °C; (--) $T > T_g$.

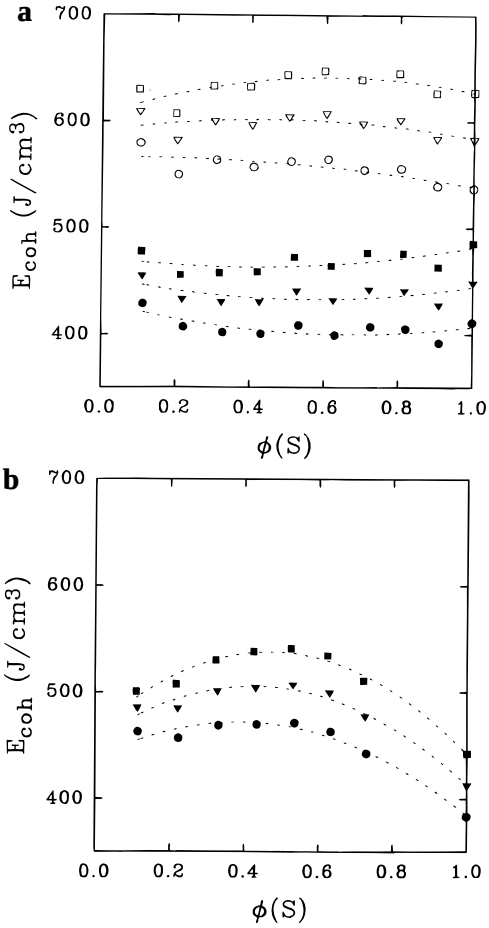

Figure 13. (a) Cohesive energy density, E_{coh} ($p = 0.1$ MPa), of ec/plasticizer mixtures versus volume fraction, $\phi(S)$, of the plasticizer according to eq 6 (filled symbols, ec-2.5/gtb; open symbols, ec-1.7/det): (■, □) 25 °C, (▼, ▽) 75 °C, (●, ○) 125 °C. (b) Cohesive energy density, E_{coh} (p = 0.1 MPa), of mixtures of ec-2.1 and tbc versus volume fraction, $\phi(S)$, of the plasticizer according to eq 6: (■) 25 °C; (▼) 75 °C; (●) 125 °C.

mixtures and show similar trends considering the different equations of state. Although it is difficult to determine accurately the respective values of the pure polymer component, the compositional dependence of E_{coh}* for ec-2.1 seems to extrapolate to a comparatively low cohesive energy density. This result is somewhat surprising in light of the fact that the increasing hydrogen-bond density should provide the greatest contribution to the increasing cohesive energy density as the degree of substitution decreases.

In contrast to the Flory theory, which assumes a reciprocal relationship between the cohesive energy and the specific volume of the system, the Simha−Somcynsky equation of state yields a relationship that depends on the volume fraction, y, of occupied lattice sites and the cell volume, yV/V*. The results are displayed in Figures 12 and 13. Following the method originally introduced by Quach and Simha,[26] a semiempirical approach was used in order to obtain y and E_{coh} at temperatures below glassy solidification. In treating the equation of state of the glass, eq 3 is retained while y is considered as an adjustable parameter to be extracted from experimental data.[27,28] At atmospheric pressure, eq 3 takes the form

$$\tilde{T} = 2y(y\tilde{V})^{-2}(1.2045-1.011(y\tilde{V})^{-2})(1-\eta) \quad (16)$$

It is reasonable to expect that the cohesive energy density can be calculated from P* below T_g as well. With this assumption, the glassy state is treated as a supercooled liquid, which is thought to have the same specific volume as the corresponding glass.

According to the compressibility data, the computed occupied volume fraction decreases with increasing plasticizer content and, of course, with temperature. If the unoccupied volume is taken as a qualitative measure for the compressibility, it is obvious that this correlation holds, at best, specifically for a given binary mixture. A striking indication of this deficiency arises when the properties of the low molecular weight components are compared. Although significantly larger values for the compressibility and the specific volume are obtained for tbc than for det, $P-V-T$ evaluation still provides a lower unoccupied volume fraction for tbc. In order to illustrate this contradictionary result, we compared the values obtained for the hole volume fraction with those calculated by the following two alternative approaches.

(a) It is a reasonable assumption that mixtures consisting of the same structural units (here, carbon backbone and ether, ester, and hydroxy groups) have an occupied incompressible volume that can be related to the respective Van der Waals hard core volume, V_{VdW}. Due to the similar carbon−oxygen ratio, only slight variations in V_{VdW} of the mixtures investigated are

Table 5. Calculated Van der Waals Volume, V_{VdW} (group contributions according to Bondi, Table 4.9[11]), Zero Point Molar Volume, V_0 (Eq. 17), and Respective Fractional Free Volume, $v_{f,0}$ (Eq. 18), Compared to the Simha−Somcynsky Unoccupied Volume Fraction, $1 - y$, Flory's "Net-Volume", v^*, and the "Flory Fractional Free Volume", $v_F = 1 - v^*/V$, at 25 °C (p = 0.1 MPa)

component	V_{VdW} (cm³/g)	V_0 (cm³/g)	$v_{f,0}$	$(1 - y)$	v^* (FOV) (cm³/g)	v_F
ec-2.5	0.566	0.736	0.180	∼0.075[a]	∼0.760	∼0.153
ec-2.1	0.559	0.727	0.162	∼0.078[a]	∼0.745	∼0.140
ec-1.7	0.552	0.718	0.148	∼0.062[a]	∼0.715	∼0.152
gtb	0.556	0.724	0.255	0.091	0.806	0.171
tbc	0.565	0.735	0.236	0.063	0.818	0.150
det	0.490	0.637	0.234	0.080	0.698	0.161

[a] According to eq 16 with estimates for V^* and T^*.

Table 6. Calculated Van der Waals Free Volume, v_f, (Eq. 19), Scaling Parameter, V^*_{SS}, Coefficient C, Coefficients a and b, and Estimate for the Hole Volume Fraction, h, According to Eq. 22 at 25 °C (p = 0.1 MPa)

component	v_f	V^*_{SS} (cm³/g)	C	a C(polymer) = 1.53 C(plasticizer) = 1.65	b	h
ec-2.5	0.369	∼0.875	1.55			0.076
ec-2.1	0.356	∼0.859	1.54	1.465	0.465	0.057
ec-1.7	0.345	∼0.822	1.49			0.040
gtb	0.428	0.9242	1.66			0.097
tbc	0.413	0.9430	1.67	1.579	0.579	0.073
det	0.411	0.7981	1.63			0.070

expected and, hence, the fractional free volume should mainly be determined by the varying polarity and hydrogen-bonding characteristics of the components (Tables 5 and 6). A good approximation for the occupied incompressible volume may be the zero point molar volume, V_0, obtained from the extrapolation of the densities of the liquid materials to 0 K. According to Bondi, V_0 and the respective fractional free volume, $v_{f,0}$, are defined as follows:[29]

$$V_0 = 1.3V_{VdW} \tag{17}$$

$$v_{f,0} = 1 - V_0/V \tag{18}$$

(b) An interesting approach with the objective of relating the Van der Waals free volume, v_f, given by eq 19, to the hole volume fraction, h ($h = 1 - y$), of the SS theory, has been introduced by Simha and Carri.[30] They coupled Eq 19 with the Simha−Wilson relation[28] (eq 20). Assuming a linear correlation function between V^* of the SS equation of state and V_{VdW} (eq 21), h can be estimated in the limit of zero reduced pressure according to eq 22.[30]

$$v_f = 1 - V_{VdW}/V \tag{19}$$

$$(1 - h)\tilde{V} = K(\tilde{T}) \tag{20}$$

$$V^* = CV_{VdW} \tag{21}$$

$$h(\tilde{T}) = av_f(T) - b \tag{22}$$

In order to calculate estimates for the hole volume fraction, h, of the components investigated, the corresponding V^* parameters were used to obtain the constants C, a, and b in our specific case. Approximating K by the average $K = 0.9568$[30] and with C (ethyl cellulose) = 1.53 and C (plasticizer) = 1.65, the coefficients a and b in eq 22 yield the values listed in Table 6.

Table 7. Characteristic Parameters, A and B, of the Atmospheric Pressure Isobar of Ec/Plasticizer Mixtures in the Range of T_u −185 °C[a]

	ec-2.5/gtb		ec-2.1/tbc		ec-1.7/det	
$w(S)$	$-A(\langle r\rangle)$	$B(\langle r\rangle)$	$-A(\langle r\rangle)$	$B(\langle r\rangle)$	$-A(\langle r\rangle)$	$B(\langle r\rangle)$
0.10	0.11367	24.912	0.12593	26.983	0.11529	24.951
0.20	0.11163	24.455	0.11664	25.226	0.11250	24.173
0.30	0.10953	23.832	0.11297	24.379	0.10974	23.437
0.40	0.10752	23.343	0.10672	23.294	0.11073	23.306
0.50	0.10737	23.109	0.10899	23.364	0.11035	22.981
0.60	0.10733	22.923	0.10852	23.066	0.11070	22.771
0.70	0.10631	22.651	0.10945	23.031	0.11075	22.583
0.80	0.10588	22.464			0.10946	22.239
0.90	0.10533	22.275			0.10902	22.065
1.00	0.10907	22.592	0.11181	22.886	0.11039	21.995

[a] T_u Values are taken from Table 4.

Although the tabulated free volumes, $v_{f,0}$, v_f, h, and v_F have different underlying definitions, their values may still be compared as has been demonstrated for h and v_f in eq 22. It is obvious that the low values evaluated for $(1 - y)$ and v_F in the case of tributyl citrate are neither consistent with the chemical constitution, which is reflected in v_f and $v_{f,0}$, nor with the free volume suggested by the compressibility (Figure 5a,b; $\kappa_{gtb} < \kappa_{tbc} < \kappa_{det}$). Nevertheless, it is worth noting that the values of $(1 - y)$ obtained generally confirm the occurrence of less unoccupied volume in polymers compared with the low molecular weight components. More significant values should, however, be provided by evaluating volume data over a markedly extended pressure range. On the other hand, there is a distinct probability that this procedure would be accomplished with a striking decrease in the accuracy of the fit.

Another interesting feature of the ec-2.1/tbc system is the apparent contradiction between the concentration dependence of the cohesive energy density and that of the occupied volume fraction since the minimum in y does hardly agree with the corresponding maximum in E_{coh}. It seems probable that these effects may have another origin, which will be discussed in the following section.

Scaling Parameters. At the limit, $P \rightarrow 0$, which is applicable to atmospheric pressure, the thermal expansion can be described by the following simple expression, with $A(\langle r\rangle)$ and $B(\langle r\rangle)$ numerics for a given $\langle r\rangle$ value:[9]

$$\ln \tilde{V} = A(\langle r\rangle) + B(\langle r\rangle)\tilde{T}^{3/2} \tag{23}$$

Applying this to nonreduced volume data, we have

$$\ln V = C + DT^{3/2} \tag{24}$$

and subsequently

$$V^*(\langle r\rangle) = \exp[C - A(\langle r\rangle)] \tag{25}$$

$$T^*(\langle r\rangle) = [B(\langle r\rangle)/D]^{2/3}$$

As well as offering an opportunity to evaluate the scaling parameters V^* and T^* solely on the basis of the atmospheric pressure isobar, the equations illustrate the close relationship between the parameters C and V^* and between D and T^*. Whereas $A(\langle r\rangle)$ and $B(\langle r\rangle)$ vary only slightly as a function of composition (Table 7, Figure 14), C and D are strongly composition dependent and longely determine the trends in V^* and T^* (Figures 9, 10, and 15a,b).

A maximum in D was found exclusively for the ec-2.1/tbc system, as is illustrated in Figure 15. Since the

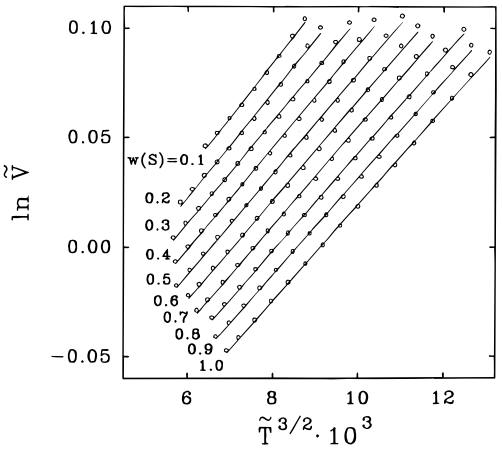

Figure 14. Reduced isobars of ethyl cellulose (DS 1.7) and diethyl tartrate and their mixtures at atmospheric pressure: (○) experiment, (—) eq 23. The curves are displaced successively on the *y*-axis by increments of ln $\tilde{V} = -0.01$ (reference curve: $w(S) = 0.1$).

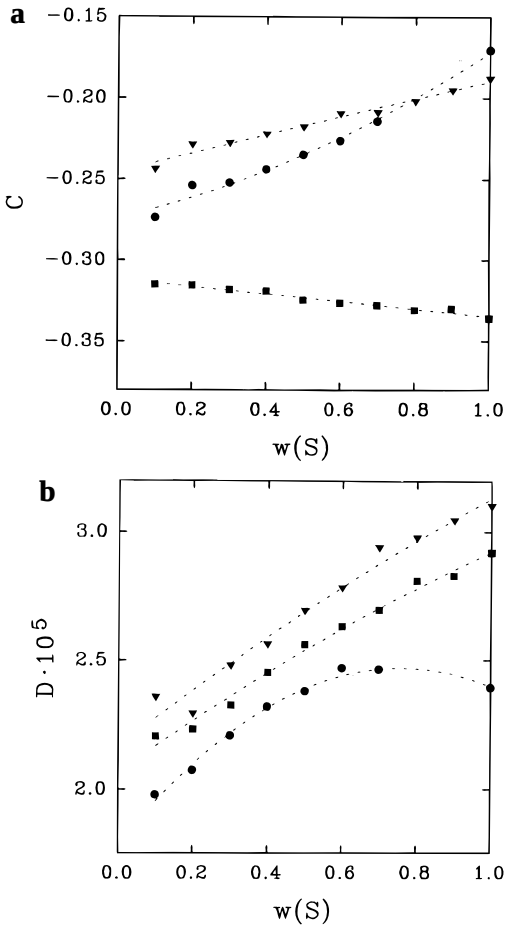

Figure 15. (a) Characteristic parameter *C* of ec/plasticizer mixtures versus weight fraction, $w(S)$, of the plasticizer (p = 0.1 MPa): (■) ec-1.7/det, (●) ec-2.1/tbc, (▼) ec-2.5/gtb. (b) Characteristic parameter *D* of ec/plasticizer mixtures versus weight fraction, $w(S)$, of the plasticizer (p = 0.1 MPa): (■) ec-1.7/det; (●) ec-2.1/tbc, shifted by −0.20; (▼) ec-2.5/gtb.

thermal expansivity, α, is proportional to D ($\alpha = \partial(\ln V)/\partial T = (3/2)DT^{1/2}$), this property seems to reflect reduced molecular attraction between the two components in the mixture compared with the pure component phases. Hence, it is fair to conclude that this behavior is also the reason for the macroscopic separation of the mixture when the solvent fraction exceeds 0.7. An indication of the nonrandomness of the distribution of plasticizer molecules has already been provided by the comparatively small T_g-depressing effect of tributyl citrate (Figure 2).

Table 8. Density, ρ (from Table VII[11]), and Cohesive Energy Density, E_{coh}, at 20 °C Calculated According to the "Direct Method" of Van Krevelen[11]

component	ρ (g/cm³)	E_{coh} (J/cm³)	component	ρ (g/cm³)	E_{coh} (J/cm³)
ec-2.5	1.123	406	gtb	1.066	363
ec-2.1	1.153	459	tbc	1.068	413
ec-1.7	1.189	520	det	1.236	686

As stated above, T^* is inversely related to D (and α) and therefore yields a convex-shaped concentration function (Figure 10). This helps to clarify the seemingly unusual concentration dependence of y (Figure12b). According to eq 4, y reflects changes in V^* and T^* and, as can easily be shown, increases as either V^* or T^* increase. It appears that although the *change* of the occupied volume fraction reflects quantitatively the increase of specific volume with increasing temperature and decreasing pressure, its *absolute* value is correlated with the inverse of the thermal expansivity [$y = y(T^*)$, $T^* \sim D^{-2/3}$, and $D \sim \alpha$]. However, the main problem in interpretating the physical meaning of the absolute values of y obtained is the lack of a realistic temperature-dependent specific volume that characterizes the perfectly occupied ($y = 1.0$) amorphous quasi-lattice. As a consequence of the limited accessible experimental pressure range, the computed fits fail to predict reliable volume data at markedly elevated pressures.

In order to discuss the physical significance of P^* (and E_{coh}), some reasonable approximations can be made despite the fact that the numerical effects of the individual scaling parameters on the shape of the $P-V-T$ surface are not easily separable from one another. In the case of the Flory theory, the internal pressure, P_i, and the cohesive energy density, E_{coh}, have an identical definition (eq 9). When the thermal pressure coefficient is taken into account, the following expression for P_i is obtained:[31]

$$P_i = \frac{P^*}{\tilde{v}^2} = \left(\frac{\partial U}{\partial V}\right)_T = T\left(\frac{\partial P}{\partial T}\right)_V - P \cong T\frac{\alpha}{\kappa} \qquad (26)$$

The corresponding relationships derived from the Simha−Somcynsky equation of state are somewhat more complex, but may generally be interpreted in the same way. Whereas V^* and T^* are determined by the isobaric thermal expansivity of the system (eqs 23−25), the internal pressure, and subsequently P^*, is closely related to the ratio of the thermal expansivity, α, to the compressibility, κ. Since the reduced specific volume has only a small effect, the origin of the composition dependence of P^* can be qualitatively deduced from the respective values of κ (Figure 5) and D (or α) (Figure 15b). For the ec-2.1/tbc system, the maximum of P^* (E_{coh}) is governed by the maximum in D and may scarcely be traced back to increased interactions between the components of the binary mixture. A similar effect is observed when the experimentally obtained values of E_{coh} of tbc and gtb are compared ($E_{coh,tbc} < E_{coh,gtb}$ since $\alpha_{tbc} < \alpha_{gtb}$). However, bearing in mind the plasticizers' chemical structure, it is reasonable to expect that the intermolecular energy per volume unit should be slightly higher in the case of tributyl citrate. This confirms an alternative calculation of E_{coh} based on functional group contributions to the theoretical heat of evaporation (Table 8).

Conclusion

The pressure−volume−temperature behavior of three structurally related polymer−solvent systems consisting of ethyl cellulose with a varying degree of substitution ($2.5 < DS < 1.7$) and an organic ester as a plasticizing component was investigated in terms of the statistical−mechanical equations of state given by the Simha−Somcynsky and the Flory−Orwoll−Vrie model. Both theories succesfully describe the experimental $P-V-T$ surface of the mixtures in the pressure range of 0−100 MPa and the temperature range of T_g−185 °C. With increasing amount of plasticizer, the glassy solidification is shifted to lower temperatures, thereby allowing the application of the equations to larger temperature ranges. In contrast to the work of Simha and co-workers,[9,16] who derived the scaling parameters V^* and T^* from the atmospheric pressure isotherm and adjusted P^* by subsequent procedures, we applied an algorithm that is capable of determining all parameters simultaneously. The computed scaling parameters obtained for the cell and the hole model vary in a similar way to one another with varying composition as their definitions are almost the same. However, it should be stressed that the actual magnitude of the SS and the FOV scaling paramaters cannot be compared directly since they depend on the effective segment and thus on the assumed $c-r$ relation.

The thermodynamic properties of ethyl cellulose and its mixtures with suitable plasticizers are strongly dependent on the polarity of the materials. The results presented for the pure polymer compounds confirm the dominant effect of hydrogen bonding on density, glass transition temperature, thermal expansivity, and compressibility.

Special attention was paid to the cohesive properties of the systems and their unoccupied volume, the latter being explicitly considered in terms of a distinct volume fraction of vacant cells, $h = 1 - y$, in the Simha−Somcynsky hole model. It turns out that, although h appears to reflect the change in the amount of unoccupied volume reasonably within the pressure and temperature range investigated, too much physical significance cannot be ascribed to its *absolute* value. Since the maximum pressure applied to the samples definitely does not exclude the occurrence of holes, the fit to the data is not capable of predicting high pressure data reliably and, consequently, fails in generating accurate absolute values for y.

The cohesive energy density is mainly governed by the P^* parameter and it has been shown that the hole model gives slightly higher values than the simple cell model. Depending on the polarity of the ethyl cellulose/plasticizer mixtures investigated, E_{coh} increases with decreasing degree of substitution of the polymer component. Focusing on mixtures with a plasticizer content of about 30%, which offer a reasonable number of isotherms for the evaluation of the scaling parameters, P^* was found to increase with the hydrogen-bond density of the systems in the order ec-2.5/gtb (P^*_{SS} = 698 MPa), ec-2.1/tbc (P^*_{SS} = 800 MPa), ec-1.7/det (P^*_{SS} = 953 MPa), and starch/glycerol ($P^*_{SS} \approx$ 1800 MPa [32]), which agrees fairly well with theoretical considerations.

It has to be emphasized that, apart from solubility experiments, which have a more or less qualitative character, the evaluation of $P-V-T$ data is the only method from which the cohesive energy of high polymers and high polymer solutions can be derived experimentally. Therefore, it serves as a most valuable tool for the determination of molecular interactions in these systems. In another paper the results obtained here are used to model the distribution of the unoccupied volume on the basis of the cohesive energy density and to discuss the solubility and the diffusion coefficients of oxygen in plasticized films of ethyl cellulose.[1]

Acknowledgment. Financial support and the permission to publish this work was given by Hoffmann-La Roche Ltd. Basel (Department Vitamins and Fine Chemicals−Product Form Development) and the Federal Institute of Technology, Zürich. We would like to thank Aqualon East BV (Rijswijk, The Netherlands) for their kind cooperation.

References and Notes

(1) Beck, M. I.; Tomka I. *J. Polym. Sci. Part B*, in press.
(2) Cohen, M. H.; Turnbull, D. *J. Chem. Phys.* **1959**, *31 (5)*, 1164.
(3) Fujita, H. *Fortschr. Hochpolym.-Forsch.* **1961**, *3*, 1.
(4) Stern, S. A.; Fang, S. M.; Frisch, H. L. *J. Polym. Sci. Part A-2* **1972**, *10*, 201.
(5) Vrentas, J. S.; Duda, J. L. *J. Polym. Sci. Part B* **1977**, *15*, 403.
(6) Vrentas, J. S.; Vrentas, C. M.; Duda, J. L. *Polym. J.* **1993**, *25 (1)*, 99.
(7) Arizzi, S.; Mott P. H.; Suter, U. W. *J. Polym. Sci. Part B* **1992**, *30*, 415.
(8) Simha, R.; Somcynsky, T. *Macromolecules* **1969**, *2 (4)*, 342.
(9) Jain, R. K.; Simha, R. *Macromolecules* **1980**, *13*, 1501.
(10) Flory, P. J.; Orwoll, R. A.; Vrij, A. *J. Am. Chem. Soc.* **1964**, *86*, 3507.
(11) Van Krevelen, D. W.; Hoftyzer, P. J. *Properties of Polymers*, 2nd ed.; Elsevier Publishing Co.: Amsterdam 1976; Chapter 7.
(12) Rodgers, P. A. *J. Appl. Polym. Sci.* **1993**, *48*, 1061.
(13) Sanchez, I. C.; Lacombe, R. H. *J. Phys. Chem.* **1976**, *80*, 2352.
(14) Panayiotou, C. G.; Sanchez, I. C. *J. Phys. Chem.* **1991**, *95*, 1090.
(15) Benczédi, D. *Dissertation No. 11203*, Swiss Federal Institute of Technology, Zürich, 1995.
(16) Simha, R.; Jain, R. K. *Colloid Polym. Sci.* **1985**, *263*, 905.
(17) Jullander, I.; Lagerström, O. In *Methods in Carbohydrate Chemistry;* Whistler, R. L., Ed.; Academic Press: New York, 1963; Vol. 3, p 303.
(18) Beck, M. I.; Tomka, I. *J. Macromol. Sci.-Phys.* **1997**, *B36* (1), 19.
(19) Kelley, F. N.; Bueche, F. *J. Polym. Sci.* **1961**, *50*, 549.
(20) Haward, R. N. *The Physics of Glassy Polymers*, Applied Science Publishers Ltd.: London, 1973.
(21) McKenna, G. B. In *Comprehensive Polymer Science* Vol. 2; Booth, C., Price, C., Eds.; Pergamon Press: New York, **1989**; Vol. 2, Chapter 10, p 311.
(22) Dimarzio, E. A.; Gibbs, J. H. *J. Polym. Sci. Part A* **1963**, *1*, 1417.
(23) Davies, R. O.; Jones, G. O. *Adv. Phys.* **1953**, *2*, 370.
(24) Beck, M. I.; Tomka, I.; Waysek, E. *Int. J. Pharm.* **1996**, *141*, 137.
(25) Lucchelli, E.; Tomka, I.; Vancso, G.; Yeh, P. L. *Polym. Bull.* **1988**, *20*, 569.
(26) Quach, A.; Simha, R. *J. Phys. Chem.* **1972**, *76*, 416.
(27) McKinney, J. E.; Simha, R. *Macromolecules* **1974**, *7*, 894.
(28) Wilson, P. S.; Simha, R. *Macromolecules* **1973**, *6*, 908.
(29) Bondi, A. *Physical Properties of Molecular Crystals, Liquids and Glasses*, John Wiley & Sons: New York, 1968.
(30) Simha, R.; Carri, G. *J. Polym. Sci. Part B* **1994**, *32*, 2645.
(31) Curro, J. G.; *J. Macromol. Sci. - Revs. Macromol. Chem. C* **1974**, *11* (2), 321.
(32) Sala, R.; Tomka, I. In *The Glassy State in Foods*; Blanshard, J. M. V., Lilleford, P. J., Eds.; Nottingham University Press: Nottingham, UK, **1993**; p 475.

MA960506V